

# Lawrence Berkeley National Laboratory

## LBL Publications

### Title

Structure Determination of Chemisorbed  $c(2 \times 2)P/Fe(100)$  using Angle-Resolved Photoemission Extended Fine Structure and Self-Consistent-Field  $X\{\alpha\}$  Scattered Wave Calculations: Comparison with  $c(2 \times 2)S/Fe(100)$

### Permalink

<https://escholarship.org/uc/item/4qn5p16k>

### Journal

Physical Review B, 55(16)

### Author

Huff, W.R.A.

### Publication Date

1996-01-22



# Lawrence Berkeley Laboratory

UNIVERSITY OF CALIFORNIA

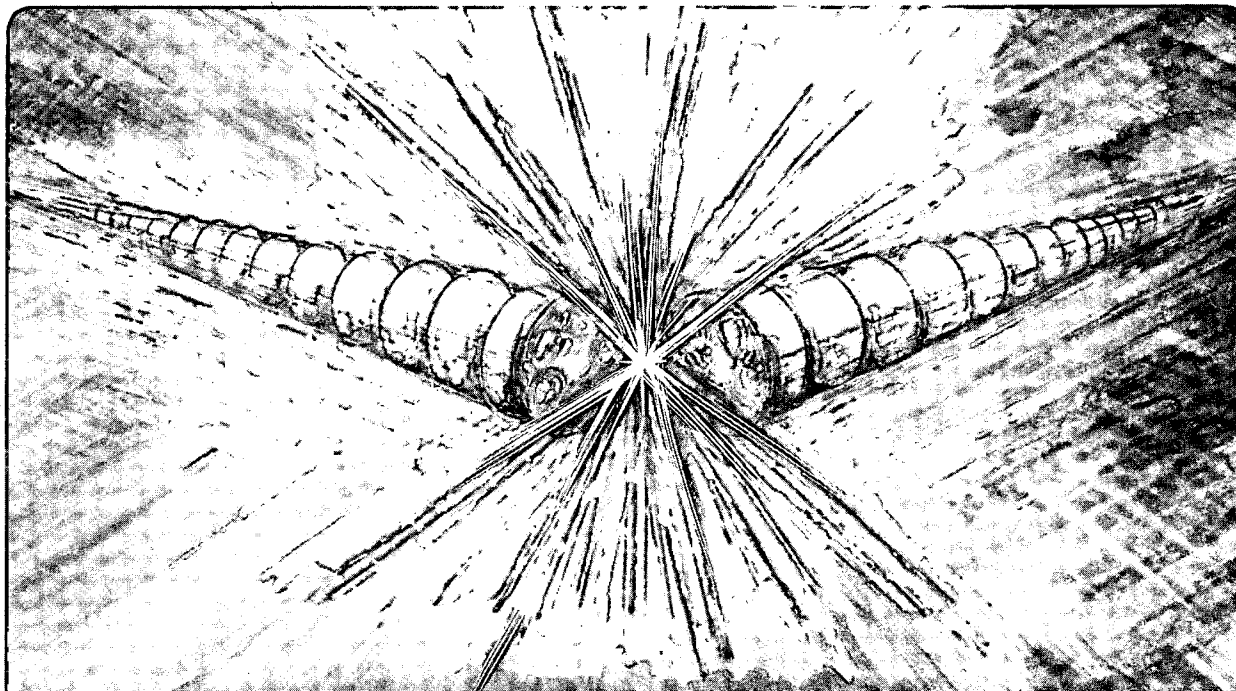
## Accelerator & Fusion Research Division

Submitted to Physical Review B

### Structure Determination of Chemisorbed $c(2 \times 2)P/Fe(100)$ using Angle-Resolved Photoemission Extended Fine Structure and Self-Consistent-Field $X\alpha$ Scattered Wave Calculations: Comparison with $c(2 \times 2)S/Fe(100)$

W.R.A. Huff, Y. Chen, X.S. Zhang, L.J. Terminello,  
F.M. Tao, Y.K. Pan, S.A. Kellar, E.J. Moler, Z. Hussain,  
H. Wu, Y. Zheng, X. Zhou, A.E. Schach von Wittenau,  
S. Kim, Z.Q. Huang, Z.Z. Yang, and D.A. Shirley

January 1996



REFERENCE COPY |  
Does Not |  
Circulate |  
Bldg. 50 Library.

LBL-38207  
COPY 1

## **DISCLAIMER**

This document was prepared as an account of work sponsored by the United States Government. While this document is believed to contain correct information, neither the United States Government nor any agency thereof, nor the Regents of the University of California, nor any of their employees, makes any warranty, express or implied, or assumes any legal responsibility for the accuracy, completeness, or usefulness of any information, apparatus, product, or process disclosed, or represents that its use would not infringe privately owned rights. Reference herein to any specific commercial product, process, or service by its trade name, trademark, manufacturer, or otherwise, does not necessarily constitute or imply its endorsement, recommendation, or favoring by the United States Government or any agency thereof, or the Regents of the University of California. The views and opinions of authors expressed herein do not necessarily state or reflect those of the United States Government or any agency thereof or the Regents of the University of California.

**Structure Determination of Chemisorbed  $c(2\times 2)P/Fe(100)$  using Angle-Resolved Photoemission Extended Fine Structure and Self-Consistent-Field  $X\alpha$  Scattered Wave Calculations: Comparison with  $c(2\times 2)S/Fe(100)$**

W.R.A. Huff,<sup>a,b</sup> Y. Chen,<sup>c</sup> X.S. Zhang,<sup>d</sup> L.J. Terminello,<sup>e</sup> F.M. Tao,<sup>f</sup> Y.K. Pan,<sup>f</sup>  
S.A. Kellar,<sup>a,b</sup> E.J. Moler,<sup>a,b</sup> Z. Hussain,<sup>a</sup> H. Wu,<sup>g</sup> Y. Zheng,<sup>h</sup> X. Zhou,<sup>c</sup>  
A.E. Schach von Wittenau,<sup>e</sup> Z. Kim,<sup>i</sup> Z.Q. Huang,<sup>j</sup> Z.Z. Yang,<sup>k</sup> and D.A. Shirley<sup>c</sup>

<sup>a</sup>Accelerator and Fusion Research Division, Ernest Orlando Lawrence Berkeley  
National Laboratory, Berkeley, CA 94720

<sup>b</sup>University of California, Department of Chemistry, Berkeley, CA 94720

<sup>c</sup>Pennsylvania State University, Department of Chemistry and Physics,  
University Park, PA 16802

<sup>d</sup>Present address: Zhejiang University, Department of Physics, Hangzhou,  
People's Republic of China

<sup>e</sup>Present address: Lawrence Livermore National Laboratory, Livermore, CA 94550

<sup>f</sup>Boston College, Department of Chemistry, Chestnut Hill, MA 02167

<sup>g</sup>Present address: University of Hong Kong, Department of Physics

<sup>h</sup>Present address: Oplink, San Jose, CA 95131

<sup>i</sup>Present address: Korea Institute of Technology, Taejon, Choongchungnam-do 300-31,  
Korea

<sup>j</sup>Present address: James Franck Institute, University of Chicago, IL 60637

<sup>k</sup>Present address: Jilin University, Institute of Theoretical Chemistry, Changchun,  
People's Republic of China

January 1996

|  |
|--|
| Light Source Note:                       |
| Author(s) Initials <i>W.R. Huff</i>      |
| Group Leader's initials <i>W.R. Huff</i> |
| Date <i>1-22-95</i>                      |

Structure Determination of Chemisorbed  $c(2 \times 2)P/Fe(100)$   
using Angle-Resolved Photoemission Extended Fine  
Structure and Self-Consistent-Field  $X\alpha$  Scattered Wave  
Calculations: Comparison with  $c(2 \times 2)S/Fe(100)$

W.R.A. Huff,<sup>a,b</sup> Y. Chen,<sup>c</sup> X.S. Zhang,<sup>d</sup> L.J. Terminello,<sup>e</sup> F.M. Tao,<sup>f</sup>  
Y.K. Pan,<sup>f</sup> S.A. Kellar,<sup>a,b</sup> E.J. Moler,<sup>a,b</sup> Z. Hussain,<sup>a</sup> H. Wu,<sup>g</sup> Y. Zheng,<sup>h</sup>  
X. Zhou,<sup>c</sup> A.E. Schach von Wittenau,<sup>e</sup> S. Kim,<sup>i</sup> Z.Q. Huang,<sup>j</sup> Z.Z. Yang,<sup>k</sup>  
and D.A. Shirley<sup>c</sup>

<sup>a</sup>Lawrence Berkeley National Laboratory, Berkeley, CA 94720

<sup>b</sup>The University of California, Dept. of Chemistry, Berkeley, CA 94720

<sup>c</sup>The Pennsylvania State University, Dept. of Chemistry and Physics,  
University Park, PA 16802

<sup>d</sup>Present address: Zhejiang University, Dept. of Physics, Hangzhou,  
People's Republic of China

<sup>e</sup>Present address: Lawrence Livermore National Laboratory,  
Livermore, CA 94550

<sup>f</sup>Boston College, Dept. of Chemistry, Chestnut Hill, MA 02167

<sup>g</sup>Present address: The University of Hong Kong, Dept. of Physics

<sup>h</sup>Present address: Oplink, San Jose, CA 95131

<sup>i</sup>Present address: Korea Institute of Technology, Taejon,  
Choongchungnam-do 300-31, Korea

<sup>j</sup>Present address: James Franck Inst., U. of Chicago, IL 60637

<sup>k</sup>Present address: Jilin University, Institute of Theoretical Chemistry,  
Changchun, People's Republic of China

## ABSTRACT

Angle-resolved photoemission extended fine structure was used to determine the structure of  $c(2 \times 2)\text{P}/\text{Fe}(100)$  for the first time. Photoemission data were collected normal to the (100) surface and  $45^\circ$  off-normal along the [011] direction at room temperature. A close analysis of the auto-regressive linear prediction based Fourier transform indicates that the P atoms adsorb in the high-coordination four-fold hollow sites. Curved-wave multiple scattering calculations confirmed the four-fold hollow adsorption site. The P atoms were determined to bond  $1.02 \text{ \AA}$  above the first layer of Fe atoms and the Fe-P-Fe bond angle is  $140.6^\circ$ . Additionally, it was determined that there was no expansion of the Fe surface. Self-consistent-field  $X\alpha$  scattered wave calculations were performed for the  $c(2 \times 2)\text{P}/\text{Fe}(100)$  and the  $c(2 \times 2)\text{S}/\text{Fe}(100)$  systems. These independent results are in excellent agreement with this P/Fe structure and the S/Fe structure previously published, confirming the ARPEFS determination that the  $\text{Fe}_1\text{-Fe}_2$  interlayer spacing is contracted from the bulk value for S/Fe but not for P/Fe. Finally, this structure is compared to structures from the literature of atomic nitrogen, atomic oxygen, and sulfur adsorbed on the Fe(100) surface.

*PACS Number: 61.14.-x, 61.14.Qp, 61.14.Rq, 68.35.Bs, 68.55.Jk*

## I. INTRODUCTION

From the viewpoint of materials science, catalysis, and magnetism, a detailed knowledge of iron and its interaction with other elements and compounds is very important. There have been many theoretical studies of the structure and embrittlement of iron grain boundaries due to the presence of phosphorus, a common impurity.<sup>1-5</sup> The electronic and magnetic properties of Fe surfaces and thin films have been studied extensively as well.<sup>6-11</sup> Egert *et al.*<sup>6</sup> seem to be the first to observe the  $c(2 \times 2)$  LEED pattern when P is adsorbed on the Fe(100) surface, but the structure determination using LEED I-V curves has not been done to date.

The structures of atomic nitrogen,<sup>12</sup> atomic oxygen,<sup>13,14</sup> and sulfur<sup>15-17</sup> adsorbed on the Fe(100) surface have been published. Using angle-resolved photoemission extended fine structure (ARPEFS), we present the first structure determination of chemisorbed  $c(2 \times 2)$ P/Fe(100). These four adsorbate structures are summarized and compared in the discussion.

Also known as scanned energy photoelectron diffraction<sup>18</sup>, ARPEFS is a technique proven to yield accurate, local structural information of atomic and molecular adsorbates on single crystal surfaces to very high precision.<sup>17,19-24</sup> In addition to determining the adsorbate structure, ARPEFS is able to detect any relaxation of the first few layers of the substrate. By analyzing the auto-regressive linear prediction (ARLP) based Fourier transform (FT),<sup>25,26</sup> the binding site and a reasonably accurate structure can be determined. This allows for a close estimate of the structure without the need for any theoretical calculations. Using this estimate as a starting point, curved-wave multiple scattering calculations can then be used to determine the structure to very high precision ( $\sim \pm 0.02 \text{ \AA}$ ).

Photoemission data were collected normal to the (100) surface and 45° off-normal along the [011] direction at room temperature. A close analysis of the ARLP based FT indicates that the P atoms adsorb in the high-coordination four-fold hollow sites. The curved-wave multiple scattering calculations which simulate the photoelectron diffraction confirmed the four-fold hollow adsorption site. By simultaneously fitting both ARPEFS data sets, the P atoms were determined to bond 1.02 Å above the first layer of Fe atoms. The Fe-P-Fe bond angle is thus 140.6°. Assuming the radius of the Fe atoms is 1.24 Å, the effective P radius is 1.03 Å. To test this fitting method, each data set was fit individually and these results were in good structural agreement.

Additionally, self-consistent-field X $\alpha$  scattered wave (SCF-X $\alpha$ -SW or X $\alpha$ -SW) calculations were performed for the c(2x2)P/Fe(100) and the c(2x2)S/Fe(100)<sup>17</sup> systems. These independent results are in excellent agreement with this P/Fe structure and the S/Fe structure previously published, confirming the ARPEFS determination that the Fe<sub>1</sub>-Fe<sub>2</sub> interlayer spacing is contracted from the bulk value for S/Fe but not for P/Fe.

## II. EXPERIMENTAL

The experiments were performed in an ultra-high vacuum chamber<sup>27</sup> at pressures  $\leq 60$  nPa using beamline 3-3 (Jumbo, the Ge(111) double crystal monochromator<sup>28</sup>) at the Stanford Synchrotron Radiation Laboratory. This beamline was chosen so that photoemission data could be acquired from the P 1s core-level which has a binding energy of 2149 eV. The photon energy was scanned from 2200 eV to 2700 eV, the energy resolution was 1.0~2.0 eV FWHM, and the degree of linear polarization was ~0.98.



The Fe crystal (6mm diameter and 2 mm thick) was cut from a boule using an electronic discharge machine. The (100) surface was oriented to  $\pm 1^\circ$  precision by Laue backscattering. Before chemical etching, the final polishing was accomplished with a 0.5  $\mu\text{m}$  mesh  $\text{Al}_2\text{O}_3$  powder. The sample was mounted on a high precision ( $x, y, z, \theta, \phi$ ) manipulator.

The crystal was cleaned by repetitive cycles of  $\text{Ar}^+$  ion sputtering (beam voltage 1.0 kV, emission current 20 mA) and subsequent annealing by electron bombardment from behind to  $\sim 970$  K. Iron undergoes a bcc to fcc phase transition at  $\sim 1180$  K so it was important not to approach this temperature. The temperature was monitored with a chromel-alumel thermocouple attached near the sample and calibrated with an infrared pyrometer. After 5 weeks of these sputter-anneal cycles, the near-surface region was depleted of C, O, and S, and the surface could be cleaned after each set of experiments by sputtering with a 0.5 kV beam voltage and annealing to only  $\sim 820$  K.

The LEED pattern of the clean surface showed a clear and sharp (1x1) pattern. The bulk contaminants C, O, and S were monitored with Auger Electron Spectroscopy (AES) using four-grid LEED optics in the retarding field mode. The surface contamination level was within the noise level of the measurements both before and after the data acquisition. The c(2x2) phosphorus overlayer was prepared by exposing the surface to  $\text{PH}_3$  gas (from Matheson Inc.) using an effusive beam doser and then annealing the sample to 770 K. In segregation studies of P in Fe, Shell and Rivière<sup>29</sup> obtained an Auger peak ratio of  $P_{\text{LMM}}(119 \text{ eV})/\text{Fe}_{\text{L}_3\text{VV}}(47 \text{ eV}) = 0.932$  whereas Egert *et al.*<sup>6</sup> who observed the c(2x2) LEED pattern obtained the Auger peak ratio  $P_{\text{LMM}}/\text{Fe}_{\text{L}_3\text{VV}} = 1.0$ . For the data presented here, the Auger peak ratio was  $P_{\text{LMM}}/\text{Fe}_{\text{L}_3\text{VV}} = 1.45$ .

The photoemission spectra were collected using an angle-resolving electrostatic hemispherical electron energy analyzer (mean radius of 50 mm) which is rotatable  $360^\circ$  around the sample's vertical axis and  $100^\circ$  around the sample's horizontal axis. The analyzer pass energy was set to 160 eV and the energy resolution was approximately 1.6 eV FWHM. The angular resolution of the double einzel input lens was  $\pm 3^\circ$ .

### III. DATA ACQUISITION AND ANALYSIS

The photoemission data were collected in two different experimental geometries. In the first data set, the photoemission angle was normal to the Fe(100) surface, i.e. the [001] direction, and the photon polarization vector was  $35^\circ$  from the surface normal. This geometry gives information which is most sensitive to the Fe atoms directly below the P atoms. It could be a first layer Fe atom if P adsorbs in an atop site or a second layer Fe atom if P adsorbs in a four-fold hollow site. If P adsorbs in a bridge site, then the data will be very different. The second set of photoemission data was collected along the [011] direction, i.e.  $45^\circ$  off normal toward the (110) crystallographic plane, and the photon polarization vector was oriented parallel to the emission angle. By taking ARPEFS data off-normal, the structure parallel to the surface is enhanced. Thus, curves from the three possible adsorption sites listed above will appear significantly different. Analyzed together, the two different experimental geometries allow for an accurate determination of interlayer spacings, bond lengths, and bond angles.

ARPEFS raw data are a series of photoemission spectra with changing photoelectron kinetic energy which was varied from 60 eV to 600 eV ( $4 \text{ \AA}^{-1}$  to  $12.5 \text{ \AA}^{-1}$ , recorded in equal  $0.1 \text{ \AA}^{-1}$  steps). Each photoemission spectrum

was a 20 eV window with the P 1s photopeak located at the center. The peak was fit with a Voigt function to model the natural linewidth as well as the experimental broadening.<sup>30</sup>

The purpose of fitting the spectra is to extract the most accurate area from the peaks to construct the  $\chi(k)$  diffraction curve containing the structural information.  $\chi(k)$  is defined by<sup>31</sup>

$$\chi(k) = \frac{I(k)}{I_0(k)} - 1 \quad (1)$$

where  $I(k)$  is the peak area plotted as a function of the peak position in  $k$ -space.  $I_0(k)$  is a smooth, slowly varying function with an oscillation frequency much lower than  $I(k)$  and stems from the contribution of the inelastic scattering processes and the varying atomic cross section. It is adequate to use a simple polynomial function of energy to fit  $I_0(k)$ .<sup>30</sup> The experimental ARPEFS data thus obtained are plotted in figure 1 along with a schematic of the respective experimental geometries. The dashed curves in figure 1 are the best-fit results from the multiple scattering modeling calculations which will be discussed later.

## A. Fourier Analysis

At this point, it is interesting to take the auto-regressive linear prediction based Fourier transform (ARLP-FT) to move from momentum space to real space. In ARPEFS, the positions of the strong peaks in ARLP-FTs from adsorbate/substrate systems can be predicted with fairly good accuracy using the single-scattering cluster (SSC) model together with the concept of strong backscattering from atoms located within a cone around

180° from the emission direction. The effective solid angle of this backscattering cone is ca. 30°-40°; it is not unique, but is operationally defined simply by opening the angle until it can account for the observed FT peaks based on the crystal geometry. Signals from scattering atoms very close to the source atom may be observable even if the scatterers lie outside the nominal backscattering cone.

These FT peaks correspond to path-length differences (PLDs),  $\Delta R_j$ , between the component of the photoemitted wave that propagates directly to the detector and the components which are first scattered by the atomic potentials within this backscattering cone.<sup>19</sup> Thus, the peak positions are

$$\Delta R_j = r_j(1 - \cos \theta_j) + \phi_j \quad (2)$$

where  $r_j$  is the bond length,  $\theta_j$  is the scattering angle (180° for exact backscattering), and  $\phi_j$  is the atomic scattering phase shift. The scattering takes place inside the crystal and the ARPEFS data must be shifted from the measured  $\chi(k_{\text{outside-crystal}})$  to  $\chi(k_{\text{inside-crystal}})$  to account for the inner potential. In ARPEFS modeling calculations, the inner potential is treated as an adjustable parameter and is typically 0 - 15 eV. The inner potential for c(2x2)S/Fe(100) was determined to be 14.5 eV.<sup>17</sup> Thus, before Fourier transformation, the ARPEFS data presented here were shifted by 14 eV to higher kinetic energy.

Without knowing anything about the structure, an analysis of the normal and off-normal ARLP-FTs can yield insight to the adsorption site as well as to the bond distance. The sharp c(2x2) LEED pattern suggests that the monolayer coverage is 50% and that the P atoms adsorb on a high symmetry site such as atop, bridge, or four-fold hollow. Using the bulk Fe

interlayer spacing, 1.43 Å, the strong peak at 4.77 Å in the [001] FT can be used as a calibration to calculate the distance between the P layer and the first Fe layer for each adsorption site. This estimation ignores the small phase shift effects. The PLDs for the strong scattering events can then be calculated and the results for each adsorption site can be compared to the [001] and [011] data FTs as is done in figure 2. The dashed vertical lines in figure 2 indicate expected peak positions for each respective geometry. The numbers with units of degrees indicate the scattering angles representative of these lines.

The calculated peak positions for the atop adsorption site are shown in figure 2a. Using the [001] FT peak at 4.77 Å for calibration, the P-Fe<sub>1</sub> interlayer spacing would be 2.39 Å. Calculating prominent PLDs shows reasonable agreement for the [001] FT except there is no way to account for the feature at 3.50 Å. Although the peak positions are in agreement, examining the [011] FT shows that an atop adsorption site is unlikely because the strongest feature in the data is the peak at 3.76 Å. The only Fe atom giving rise to this PLD would be at a scattering angle  $\theta_j = 85^\circ$ . Since ARPEFS is dominated by backscattering events,<sup>19,25</sup> the data peak at 7.57 Å should dominate the FT if P adsorbs in an atop geometry.

When considering a bridge adsorption site, there are two possible P-Fe<sub>1</sub> interlayer spacings, depending on which atom one chooses for calibration of the 4.77 Å [001] data peak. Figure 2b indicates a spacing of 2.17 Å obtained if one believes that scattering from the *first* layer Fe atoms gives rise to this peak. Figure 2c indicates a spacing of 0.74 Å obtained if one believes that scattering from the *second* layer Fe atoms gives rise to this peak. In each case, only one of two possible bridge sites can be occupied with a c(2x2) LEED pattern. These sites are degenerate for the [001] FT but

become distinct for the [011] FT. For the off-normal case, the strong backscattering peak will be either from a first layer Fe atom or from a second layer Fe atom. Due to the symmetry of the (100) crystal face, each bridge site is energetically degenerate. Thus, in an experimental situation, domains of each will occur and [011] ARPEFS data from  $\theta = 45^\circ$ ,  $\phi = 0^\circ$  would be identical to ARPEFS data where  $\theta = 45^\circ$ ,  $\phi = 90^\circ$ . The FT would show peaks from each domain. Therefore, if P adsorbed onto a bridge site, many more peaks would be expected in the [011] FT than are actually there. What this discussion implies is that ARPEFS is unable to distinguish the two domains of c(2x2) from a p(1x1) coverage in which both bridge sites were occupied equally. Unless, of course, the adsorbate-adsorbate interaction significantly effects the adsorbate-substrate bonding in the denser coverage.

As with the bridge site, two P-Fe<sub>1</sub> interlayer spacings are possible with the four-fold hollow site. If the data peak at 4.77 Å is due to scattering from a *first* layer Fe atom, then the layer spacing would be 1.96 Å. These calculated PLDs are shown in figure 2d. However, if this were the correct geometry, an intense peak due to backscattering from the second layer Fe atoms is expected at 6.79 Å. Additionally, the [011] FT would be dominated by a backscattering PLD at 5.22 Å. The scattering angle for the line at 3.19 Å would be 98° which is not expected to be so strong as described above.

Alternatively, if the P adsorbs in a four-fold hollow site and the data peak at 4.77 Å is due to backscattering from the *second* layer Fe atoms, then the P-Fe<sub>1</sub> interlayer spacing would be 0.95 Å. These calculated PLDs are shown in figure 2e. For this proposed geometry, the calculated PLDs are in good agreement with the data and the scattering angles are reasonable for the relative strengths of each peak.

In fact, from the structure analysis of  $c(2 \times 2)S/Fe$ ,<sup>15-17</sup> it is expected that the P atoms adsorb in the four-fold hollow sites and are  $\sim 1 \text{ \AA}$  above the first layer Fe atoms. It is possible to extend this estimate by calibrating the  $P-Fe_1$  interlayer spacing to each strong data peak and then averaging the results. Doing this estimation, the  $P-Fe_1$  interlayer spacing would be  $1.19 \text{ \AA}$ . Noting that this distance is significantly expanded over the  $S/Fe$  value of  $1.09 \text{ \AA}$ <sup>17</sup> and that this process neglects phase shifts, one should realize that  $1.19 \text{ \AA}$  is probably too large.

Modeling calculations to be described in the next section are necessary to obtain highly precise bond distances. However, with no modeling calculations, it has already been determined that P adsorbs in the high coordination four-fold hollow sites and the  $P-Fe_1$  interlayer spacing is between  $0.95 \text{ \AA}$  and  $1.19 \text{ \AA}$ . The ARLP-FTs for both the [001] and the [011] data sets are presented in figure 3. Also shown in figure 3 is a schematic of the crystal with the backscattering cone for each emission direction superimposed; the labeled atoms correspond to labeled peaks in each FT. The solid lines indicate the scattering atoms for [001] photoemission while the dashed lines indicate the scattering atoms for [011] photoemission. Peaks arise in the FT due to scattering from atoms up to five layers below the emitting atoms. The depth sensitivity of ARPEFS has been described previously<sup>32</sup> and was found to be enhanced by multiple-scattering effects.

## B. Multiple Scattering Analysis

Modeling calculations were performed to simulate the ARPEFS  $\chi(k)$  curve and obtain a structure more precise than yielded by the FT analysis. Using the single-scattering model of ARPEFS,<sup>19,31</sup>  $\chi(k)$  can be written as

$$\chi(k) = \sum_j A_j(k) \cos \left[ k(R_j - R_j \cos \theta_j) + \phi_j \right] \quad (3)$$

where  $A_j(k)$  contains experimental geometry factors including the photon polarization direction and the electron emission direction as well as the scattering amplitude, aperture integration, and thermal averaging.

A new code developed by Chen, Wu, and Shirley<sup>33</sup> based on the Rehr-Albers formalism<sup>34</sup> was used for the multiple-scattering spherical-wave calculations presented here. This new code differs from the Kaduwela/Fadley code<sup>35</sup> and is sufficiently fast that multi-curve fitting calculations can be performed.

The calculations require both structural and nonstructural input parameters. The initial structural parameters were determined from the FT analysis. The nonstructural parameters included were the initial state, the atomic scattering phase shifts, the crystal temperature, the inelastic mean free path, the emission and polarization directions, the electron analyzer acceptance angle, and the inner potential. The fitting procedure allowed the structure to vary as well as the inner potential such that a best fit was obtained.

To account for vibration effects of the bulk atoms, the mean square relative displacement (MSRD) was calculated using equation (33) by Sagurton *et al.*<sup>36</sup>

$$\langle u_i^2 \rangle \propto \frac{1}{M_i \theta_{D,i}} \left( 1 + \frac{cT^2}{\theta_{D,i}^2} \dots \right) \quad (4)$$



where  $M_i$  is the atomic mass,  $\theta_{D,i}$  is the correlated Debye temperature,  $T$  is the sample temperature, and  $c$  is a coefficient that varies slowly with temperature. For calculating the MSRD of the bulk Fe atoms,  $\theta_{D,i}$  was set to 400 K.

Accounting for the surface atomic vibration is not as straightforward. The relation between the MSRD and different atomic masses has been given by Allen *et al.*<sup>37</sup>

$$\langle u_i^2 \rangle \sqrt{M_i} = \langle u_j^2 \rangle \sqrt{M_j} \quad (T \approx 0 \text{ K}) \quad (5)$$

$$\langle u_i^2 \rangle = \langle u_j^2 \rangle \quad (T \rightarrow \infty) \quad (6)$$

Correlating equations (5) and (6) with equation (4), an effective surface atomic mass is introduced such that

$$\langle u_{i,\text{bulk}}^2 \rangle \sqrt{M_{i,\text{bulk}}} \equiv \langle u_{j,\text{surface}}^2 \rangle \sqrt{M_{j,\text{effective}}} \quad (7)$$

where  $M_{j,\text{effective}} = M_{j,\text{surface}}$  if  $T/\theta_{D,i} \ll 1$  or  $M_{j,\text{effective}} = M_{j,\text{bulk}}$  if  $T/\theta_{D,i} > 1$ . For  $T/\theta_{D,i} \approx 1$ ,  $M_{j,\text{effective}}$  is allowed to vary between the surface and bulk atomic masses. For this study where  $T = 300 \text{ K}$  and  $\theta_{D,i} = 400 \text{ K}$ , it was found that the calculated  $\chi(k)$  diffraction curve was insensitive to the surface atomic mass, so  $M_{j,\text{effective}}$  was set to the atomic mass of P, 31 a.u.

The atomic-scattering phase shifts were calculated in situ by using the atomic potentials tabulated by Moruzzi *et al.*<sup>38</sup> The emission and polarization directions and the electron analyzer acceptance angle were set to match the experiment as described earlier. The inelastic mean free path (IMFP) was included using the exponential damping factor  $e^{-t/\lambda}$  where  $\lambda$  was calculated using the Tanuma, Powell, and Penn (TPP-2) formula.<sup>39</sup> The

IMFP calculation is important in obtaining a close fit to the data and in determining the depth sensitivity of ARPEFS. The TPP-2 formula seems to be the most accurate method to determine the IMFP, especially below 200 eV.

The 'multi-curve fitting' feature means that multiple data curves can be fit simultaneously as explained later. Figure 1 illustrates the best fit (dashed lines) to both the [001] and the [011] ARPEFS data sets (solid lines) by simultaneous fitting. For these fits, a 76 atom cluster was used and the P-Fe<sub>1</sub> interlayer spacing was determined to be 1.02(2) Å. The inner potential was 15.0 eV. The fitting also determined that there was no relaxation of the first or second Fe layers from the bulk 1.43 Å interlayer spacing.

Each data curve was also fit individually to compare the results. For the [001] individual fit, a 76 atom cluster was used and the P-Fe<sub>1</sub> interlayer spacing was determined to be 1.02(2) Å. For the [011] individual fit, a 75 atom cluster was used and the P-Fe<sub>1</sub> interlayer spacing was determined to be 1.01(2) Å. The inner potential was the same as with the simultaneous fits. Neither of the individual fits showed any relaxation of the first two Fe layers. These results confirm the validity of the multi-curve fitting method.

Finally, an attempt was made to fit the ARPEFS data using an atop adsorption site and a bridge adsorption site. For each site, the [001] and [011] curves were fit simultaneously. The results are presented in figure 4.

Simple visual inspection is sufficient to rule out the atop and bridge adsorption sites. The [001] atop fit is quite good, as is expected due to the symmetry similarities with the four-fold hollow site. When viewing off-normal, however, this symmetry is broken. This is shown by the [011] fit which is better for the four-fold hollow site than for the atop site (e.g., at

$\sim 6.5 \text{ \AA}^{-1}$  and  $\sim 9 \text{ \AA}^{-1}$ ). The bridge best fits are not competitive with the other two possible sites, especially when viewing off-normal.

These comparisons further prove that the P atoms adsorb in the four-fold hollow sites as concluded from the FT analysis. Additionally, they illustrate the importance of acquiring ARPEFS data in at least two different emission directions to be certain of the adsorption site. The four-fold hollow adsorption site and the P-Fe<sub>1</sub> interlayer spacing for this c(2x2)P/Fe(100) structure correlate well with the structure for chemisorbed c(2x2)S/Fe(100).<sup>15-17</sup>

### C. Discussion of Error

The best fit is determined by an  $R$ -factor minimization. A three-step fitting process is used to determine the true  $R$ -factor minimum to prevent convergence to a local minimum. The initial coarse-fitting minimizes the  $\tilde{R}$ -factor,  $\tilde{R} = R_a$  where

$$R_a = \frac{\sum_i [\chi_{i,c}(k) - \chi_{i,e}(k)]^2}{\sum_i [\chi_{i,c}^2(k) + \chi_{i,e}^2(k)]} \quad (8)$$

using a simple net search.<sup>33</sup>  $\chi_{i,c}(k)$  and  $\chi_{i,e}(k)$  are the points in the calculated and experimental  $\chi(k)$  curves respectively. Second, the code again minimizes  $\tilde{R} = R_a$  using the Downhill Simplex Method in Multidimensions.<sup>40</sup> Finally, the code minimizes  $\tilde{R} = R$  where

$$R = \frac{\sum_i [\chi_{i,c}(k) - \chi_{i,e}(k)]^2}{\sum_i \chi_{i,e}^2(k)} \quad (9)$$

using the Nonlinear Marquardt Method.<sup>40</sup>

When using the multi-curve fitting feature,  $\tilde{R}$ -factors from each fit must be considered. For this, the sum of the individual  $\tilde{R}$ -factors,  $\tilde{R}_{\text{total}}$ , is used. Thus, if fitting  $N$  ARPEFS curves simultaneously, then

$$\tilde{R}_{\text{total}} = \sum_j \frac{1}{N} \tilde{R}_j \quad (10)$$

Note that the code is flexible such that a weighted sum could be used if justification could be made for giving preference to the  $\tilde{R}$ -factor of one ARPEFS curve over another.

While fitting, the largest effects stem from changes in the inner potential and the P-Fe<sub>1</sub> interlayer spacing. Figure 5 shows a contour plot of the  $R$ -factor as the inner potential and P-Fe<sub>1</sub> interlayer spacing are varied. Analysis of figure 5 indicates that the precision of ARPEFS is  $\sim \pm 0.02$  Å, but only if the inner potential is known very well. If, however, the inner potential is allowed to float without constraint, the precision of ARPEFS drops to  $\sim \pm 0.03$  Å.

#### IV. SCF-X $\alpha$ -SW Calculations

The chemisorption structure of c(2x2)P/Fe(100) and c(2x2)S/Fe(100)<sup>17</sup> from the experimental determination may be further confirmed by theoretical calculations in an appropriate model. In this

section, we present SCF-X $\alpha$ -SW (or X $\alpha$ -SW) calculations on two atomic clusters, PFe<sub>9</sub> and SFe<sub>9</sub>, which represent the two chemisorption systems P/Fe and S/Fe, respectively.

The SCF-X $\alpha$ -SW formalism developed by Slater<sup>41</sup> and Johnson<sup>42,43</sup> seems to be a convenient compromise between the need for rigorous calculations and the limitations of computing resources. The SCF equation is solved numerically. Basis sets are utilized only in the sense that there is a choice of maximum  $\ell$  value allowed on each center. The numerical solution is made possible by the X $\alpha$  approximation for the exchange contribution to the total potential and the muffin-tin approximation for molecular potential and charge densities. Studies of a range of molecular properties have shown that this method has better performance than semiempirical MO methods and gives results of roughly double-zeta *ab initio* quality.<sup>44-49</sup> The tremendous orbital sizes in our clusters make *ab initio* methods virtually impossible to apply and so the X $\alpha$ -SW method is the highest level of theory practically available for this work. In fact, the X $\alpha$ -SW method is particularly appropriate because of the high symmetry of the clusters for the calculations.

Due to the limitations of the muffin-tin approximation, the X $\alpha$ -SW method may not provide a very accurate calculation of reaction energetics such as the adsorption energy of the P/Fe or S/Fe system. However, the error introduced by the muffin-tin approximation can be overcome to some extent by the use of overlapping atomic spheres.<sup>50</sup> We therefore expect that the relative changes of the total energy can be described to desirable accuracy, especially those involved in small structural variations near the equilibrium positions. Of course, the standard parameters should be used for

this purpose and the predicted equilibrium structures should not be sensitive to the values of the parameters.

All standard non-empirical parameters for the calculations were used. The radii of atomic spheres were chosen according to Norman<sup>51</sup> and the  $\alpha$  exchange parameters were taken from Schwarz's<sup>52</sup> tabulations. In the intersphere and outersphere regions, an average value of  $\alpha$ , obtained from a valence-weighted average of the  $\alpha$ 's for the atoms in the cluster, is employed. Figure 6 shows the structures of the two clusters PFe<sub>9</sub> and SFe<sub>9</sub>. The overall symmetry for each cluster is C<sub>4v</sub>. The four Fe atoms in the top layer are labeled by Fe<sub>1</sub> and the five Fe atoms in the second layer are labeled by Fe<sub>2</sub>. The distance of the adsorbed atom P (or S) to the plane formed by the Fe<sub>1</sub> atoms is P-Fe<sub>1</sub> (or S-Fe<sub>1</sub>) and the distance between the first and the second layers of Fe atoms is Fe<sub>1</sub>-Fe<sub>2</sub>. The total energies of the clusters were calculated at several P-Fe<sub>1</sub> (S-Fe<sub>1</sub>) distances embracing the experimental equilibrium distance while the Fe<sub>1</sub>-Fe<sub>2</sub> interlayer distance was kept at the experimental value. The total energy for a different Fe<sub>1</sub>-Fe<sub>2</sub> interlayer distance was also calculated at the experimental P-Fe<sub>1</sub> (S-Fe<sub>1</sub>) distance to compare the structural difference in the Fe<sub>1</sub>-Fe<sub>2</sub> layer between the P/Fe and the S/Fe systems. The calculation results are presented in tables 1 and 2 for PFe<sub>9</sub> and SFe<sub>9</sub>, respectively.

It is seen in table 1 that the P-Fe<sub>1</sub> interlayer distance at the energy minimum is around 1.01 Å with the Fe<sub>1</sub>-Fe<sub>2</sub> interlayer distance set at the bulk value of 1.43 Å. This result is consistent with the experimentally obtained structure. Table 2 similarly shows good agreement between the calculations and experiment for the S/Fe<sup>17</sup> system where the S-Fe<sub>1</sub> interlayer distance at the energy minimum is around 1.09 Å with the Fe<sub>1</sub>-Fe<sub>2</sub> interlayer distance set at the experimentally determined value of 1.40 Å.

These calculation results confirm the ARPEFS determination that the Fe<sub>1</sub>-Fe<sub>2</sub> interlayer spacing is contracted from the bulk value for S/Fe but not for P/Fe. If the Fe<sub>1</sub>-Fe<sub>2</sub> interlayer spacing is contracted to 1.40 Å for the P/Fe system, the total energy is raised by 1.39 eV. Similarly, if the Fe<sub>1</sub>-Fe<sub>2</sub> interlayer spacing is fixed at the 1.43 Å bulk value for the S/Fe system, the total energy is raised by 3.82 eV.

## V. DISCUSSION

In this section, the structure determined here for c(2x2)P/Fe(100) is compared with atomic c(2x2)N/Fe(100),<sup>12</sup> atomic p(1x1)O/Fe(100),<sup>13,14</sup> and c(2x2)S/Fe(100)<sup>15-17</sup>. These four elements border each other on the periodic table and their interaction with iron is very important in materials science, catalysis, and magnetism.

In table 3, a summary of these four structures is presented along with the structure of the clean Fe(100) surface.<sup>17,53</sup> The structure of atomic O adsorbed on the Fe(100) surface is interesting because the coverage is p(1x1), unlike atomic N, P, or S. Also, using first principles calculations, Chubb and Pickett<sup>14</sup> predict a very large expansion of the first layer Fe atoms. A smaller (by a factor of three) but significant expansion was experimentally determined by Legg *et al.* using LEED.<sup>13</sup> Figure 7 shows a schematic of both proposed oxygen structures (experiment on left, theory on right) as well as the structures for N, P, and S. Because of its ability to accurately determine the near-surface reconstruction of the substrate, ARPEFS should be used to study the p(1x1)O/Fe(100) structure.

## VI. CONCLUSION

Angle-resolved photoemission extended fine structure was used to determine the structure of  $c(2 \times 2)P/Fe(100)$  for the first time. Photoemission data were collected normal to the (100) surface and  $45^\circ$  off-normal along the [011] direction at room temperature. A close analysis of the ARLP based FT indicates that the P atoms adsorb in the high-coordination four-fold hollow sites. The FT analysis also allowed the bond distances to be estimated with surprisingly high accuracy. The curved-wave multiple scattering calculations which simulate the photoelectron diffraction confirmed the four-fold hollow adsorption site. By simultaneously fitting both ARPEFS data sets, the P atoms were determined to bond  $1.02(2)$  Å above the first layer of Fe atoms. The Fe-P-Fe bond angle is thus  $140.6^\circ$ . Assuming the radius of the Fe atoms is  $1.24$  Å, the effective P radius is  $1.03$  Å. The inner potential was  $15.0$  eV. It was also determined that there was no relaxation of the first or second Fe layers from the bulk  $1.43$  Å interlayer spacing. To test this fitting method, each data set was fit individually and these results were in good structural agreement.

Additionally, self-consistent-field  $X\alpha$  scattered wave calculations were performed for the  $c(2 \times 2)P/Fe(100)$  and the  $c(2 \times 2)S/Fe(100)$ <sup>17</sup> systems. These independent results are in excellent agreement with this P/Fe structure and the S/Fe structure previously published, confirming the ARPEFS determination that the  $Fe_1$ - $Fe_2$  interlayer spacing is contracted from the bulk value for S/Fe but not for P/Fe.



## **ACKNOWLEDGMENTS**

This work was supported by the Director, Office of Energy Research, Office of Basic Energy Sciences, Chemical Sciences Division of the U.S. Department of Energy under Contract No. DE-AC03-76SF00098. It was performed at the Stanford Synchrotron Radiation Laboratory which is supported by the Department of Energy's Office of Basic Energy Sciences.

## TABLES

- Table 1: Variations of the total energy and the relative energy of PFe<sub>9</sub> with the P-Fe<sub>1</sub> interlayer distance from X $\alpha$ -SW calculations (Fe<sub>1</sub>-Fe<sub>2</sub> was fixed at 1.43 Å). The last row lists the calculated energy with Fe<sub>1</sub>-Fe<sub>2</sub> fixed at 1.40 Å.
- Table 2: Variations of the total energy and the relative energy of SFe<sub>9</sub> with the S-Fe<sub>1</sub> interlayer distance from X $\alpha$ -SW calculations (Fe<sub>1</sub>-Fe<sub>2</sub> was fixed at 1.40 Å). The last row lists the calculated energy with Fe<sub>1</sub>-Fe<sub>2</sub> fixed at 1.43 Å.
- Table 3: Structures of clean Fe(100), c(2x2)N/Fe(100), p(1x1)O/Fe(100), c(2x2)P/Fe(100), and c(2x2)S/Fe(100). For the Fe<sub>1</sub>-Fe<sub>2</sub> interlayer spacing, the percent expansion from the 1.43 Å bulk value is indicated. For O/Fe, the upper value indicates the experimental results<sup>13</sup> while the lower value indicates the theoretically predicted structure.<sup>14</sup> "X" indicates the adsorbate.

Table 1: SCF-X $\alpha$ -SW Calculation Results for PFe<sub>9</sub>

| P-Fe <sub>1</sub> Interlayer Spacing (Å) | Total Energy (eV) | $\Delta E$ (eV) |
|--|-------------------|-----------------|
| 1.06                                     | -318411.46        | 1.89            |
| 1.04                                     | -318412.48        | 0.87            |
| 1.01                                     | -318413.35        | 0               |
| 0.99                                     | -318410.35        | 3.00            |
| 1.01                                     | -318411.97        | 1.38            |

Table 2: SCF-X $\alpha$ -SW Calculation Results for SFe<sub>9</sub>

| S-Fe <sub>1</sub> Interlayer Spacing (Å) | Total Energy (eV) | $\Delta E$ (eV) |
|--|-------------------|-----------------|
| 1.14                                     | -319983.03        | 2.39            |
| 1.12                                     | -319984.57        | 0.85            |
| 1.09                                     | -319985.42        | 0               |
| 1.07                                     | -319984.40        | 1.02            |
| 1.04                                     | -319982.77        | 2.65            |
| 1.09                                     | -319981.60        | 3.82            |

Table 3: Adsorbate Structure on an Fe(100) Substrate

|  | Clean Surface             | Atomic Nitrogen | Atomic Oxygen <sup>b</sup>  | Phosphorus | Sulfur       |
|--|---------------------------|-----------------|-----------------------------|------------|--------------|
| Coverage                                 | --                        | c(2x2)          | p(1x1)                      | c(2x2)     | c(2x2)       |
| $r_{\text{eff}}[X]$ (Å)                  | --                        | 0.59            | 0.78                        | 1.03       | 1.06         |
| $r_{\text{eff}}[\text{Fe}]$ (Å)          | 1.24                      | 1.24            | 1.24                        | 1.24       | 1.24         |
| $d_{\perp}[X-\text{Fe}_1]$ (Å)           | --                        | 0.27            | 0.48<br>0.38                | 1.02       | 1.09         |
| $d_{\perp}[\text{Fe}_1-\text{Fe}_2]$ (Å) | 1.41 (-1.4%) <sup>a</sup> | 1.54 (+7.7%)    | 1.54 (+7.7%)<br>1.76 (+23%) | 1.43       | 1.40 (-2.1%) |
| $d_{\perp}[\text{Fe}_2-\text{Fe}_3]$ (Å) | 1.43                      | 1.43            | 1.43                        | 1.43       | 1.46 (+2.1%) |
| $d_{\perp}[X-\text{Fe}_2]$ (Å)           | --                        | 1.81            | 2.02<br>2.14                | 2.45       | 2.49         |
| Bond Angle<br>Fe-X-Fe                    | --                        | 164.8°          | 153.3°<br>158.7°            | 140.6°     | 123.4°       |

<sup>a</sup>Percent expansion from the bulk 1.43 Å value.

<sup>b</sup>Upper value from reference 13; Lower value from reference 14.

## FIGURES

- Figure 1: ARPEFS  $\chi(k)$  data for c(2x2)P/Fe(100) in the [001] and [011] directions. Also, schematics of each experimental geometry are shown. The dashed lines are the best-fit multiple scattering modeling calculation results obtained by fitting both data sets simultaneously.
- Figure 2: ARLP based FTs of the ARPEFS [001] data (left column) and [011] data (right column). The dashed vertical lines indicate the expected peak positions based on calibration to the [001] peak at 4.77 Å for a) atop,  $d_{\perp} = 2.39$  Å; b) bridge,  $d_{\perp} = 2.17$  Å; c) bridge,  $d_{\perp} = 0.74$  Å; d) four-fold hollow,  $d_{\perp} = 1.96$  Å; e) four-fold hollow,  $d_{\perp} = 0.95$  Å. The numbers with units of degrees indicate the scattering angles representative of each respective line. Considering both the expected positions and the scattering angles, e) is most likely the closest estimation to the true structure.
- Figure 3: ARLP based FTs of the ARPEFS [001] data (solid line) and [011] data (dashed line). A model of the lattice with the backscattering cones for each emission direction indicates the scattering atoms corresponding to the FT peaks.
- Figure 4: Best fit (dashed lines) to the [001] and [011] ARPEFS data by assuming an atop adsorption site or a bridge adsorption site.
- Figure 5: Contour plot showing how the  $R$ -factor varies with the P-Fe<sub>1</sub> interlayer spacing and the inner potential when simultaneously fitting the [001] and [011] ARPEFS data.
- Figure 6: Structure of the two clusters PFe<sub>9</sub> and SFe<sub>9</sub> used for the X $\alpha$ -SW calculations.
- Figure 7: Schematics of the structures of atomic c(2x2)N/Fe(100), atomic p(1x1)O/Fe(100) (experiment on left, theory on right), c(2x2)P/Fe(100), and c(2x2)S/Fe(100).

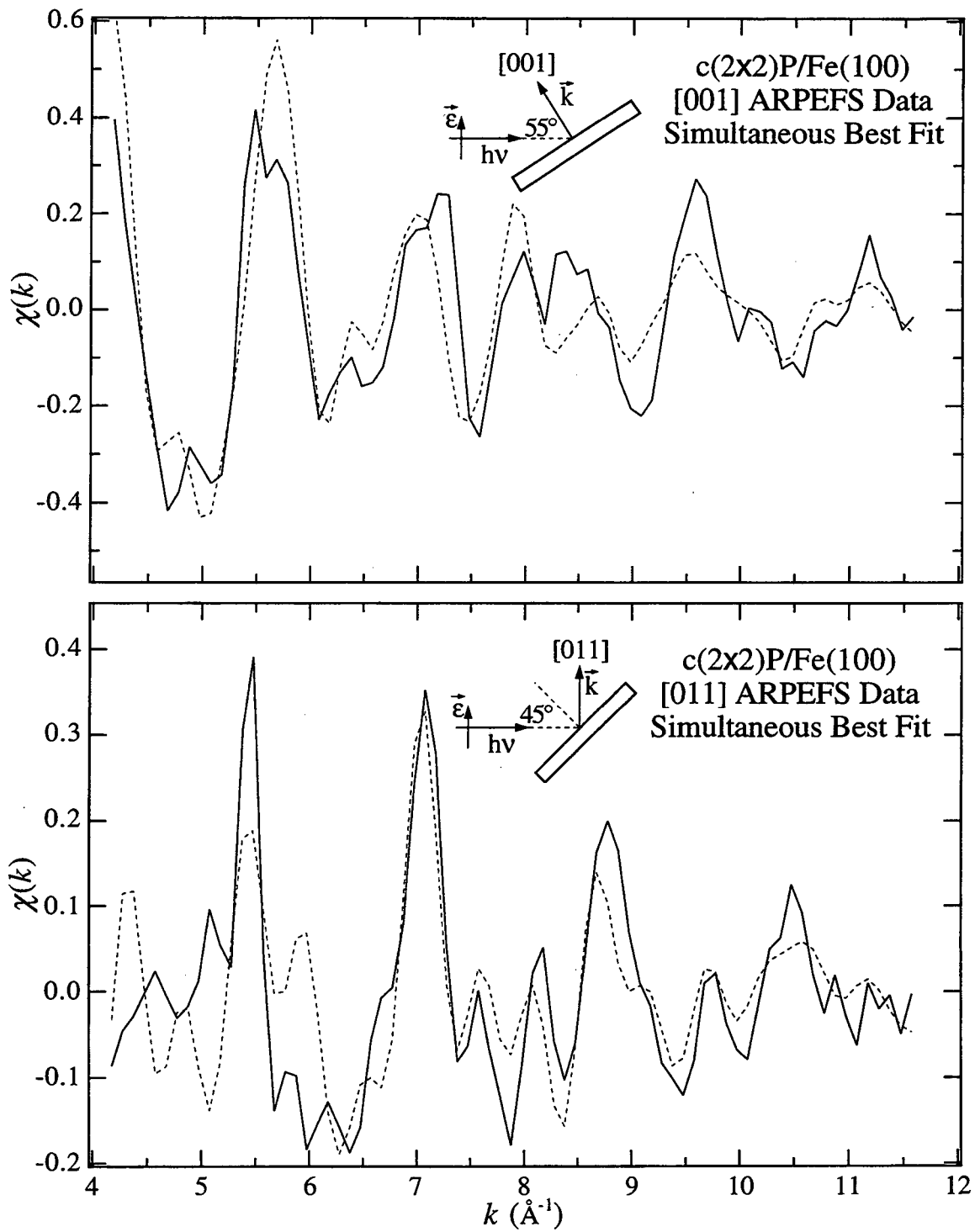


Figure 1

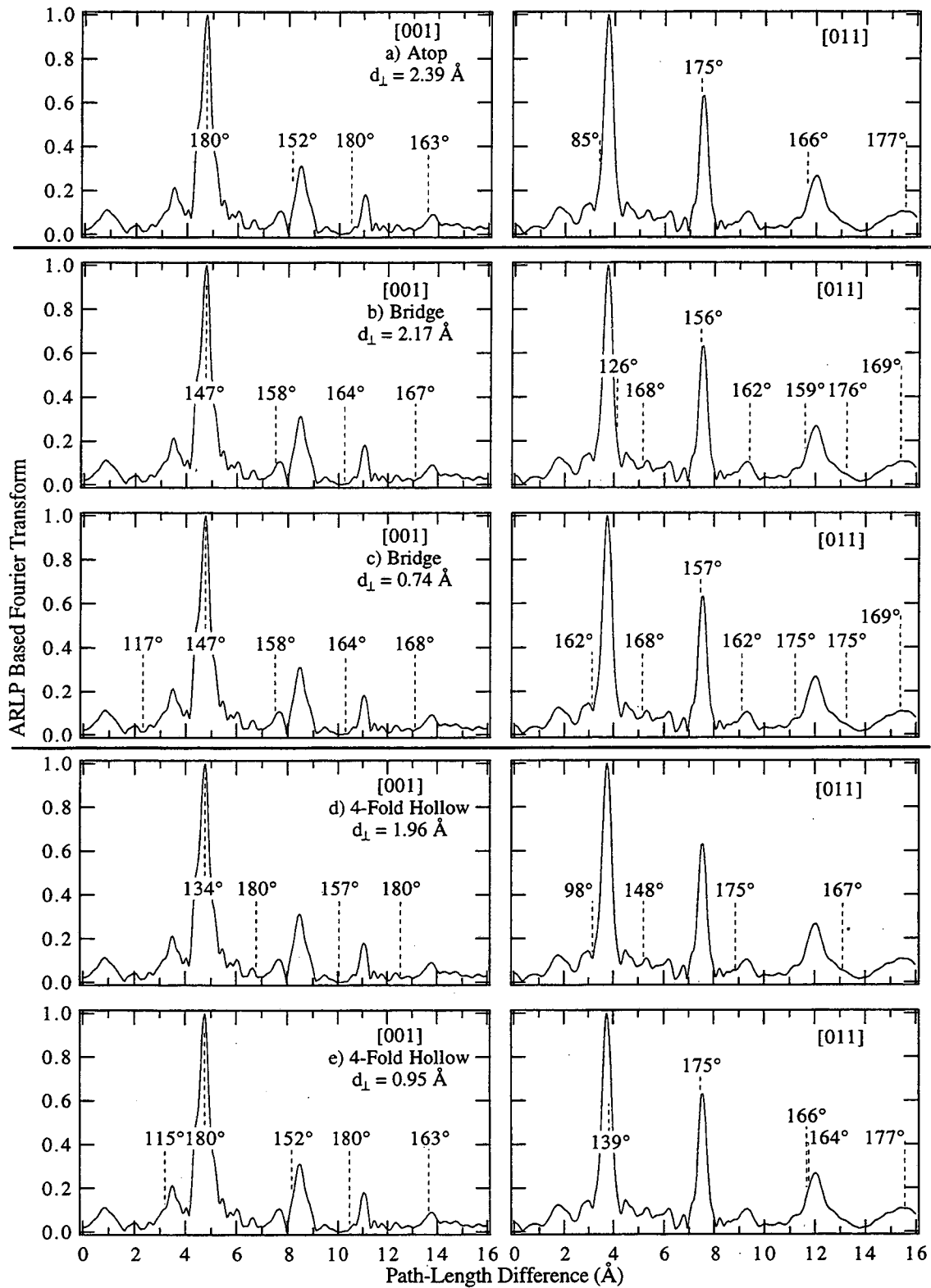


Figure 2



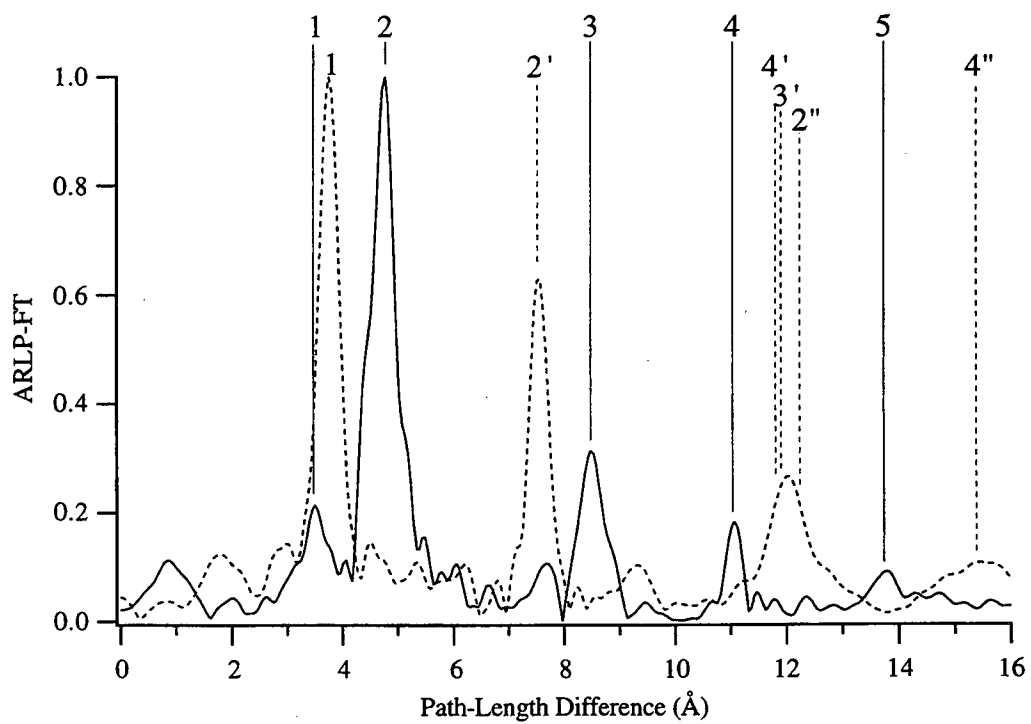
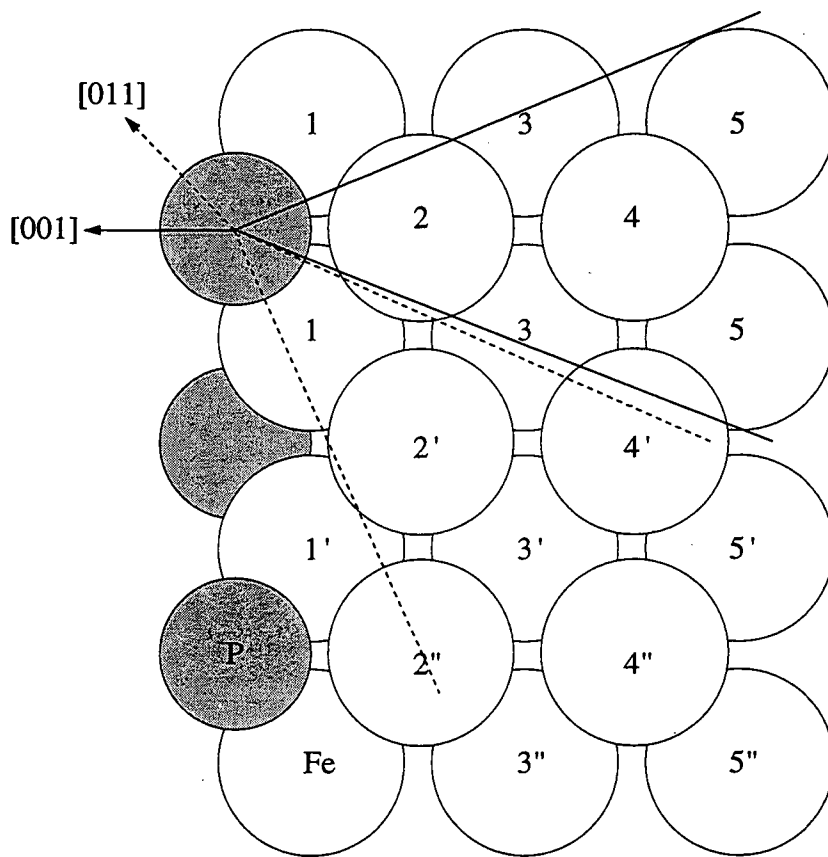


Figure 3

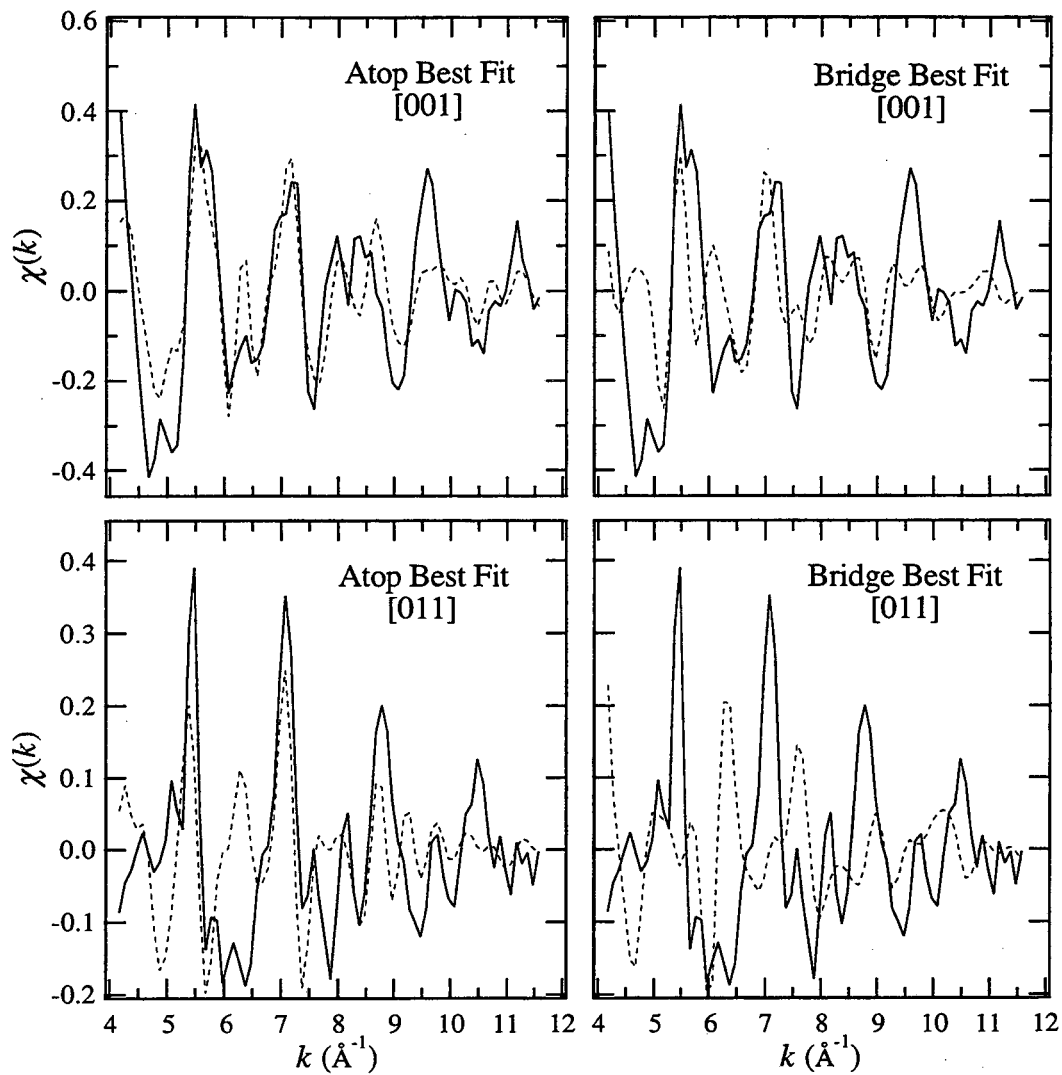


Figure 4

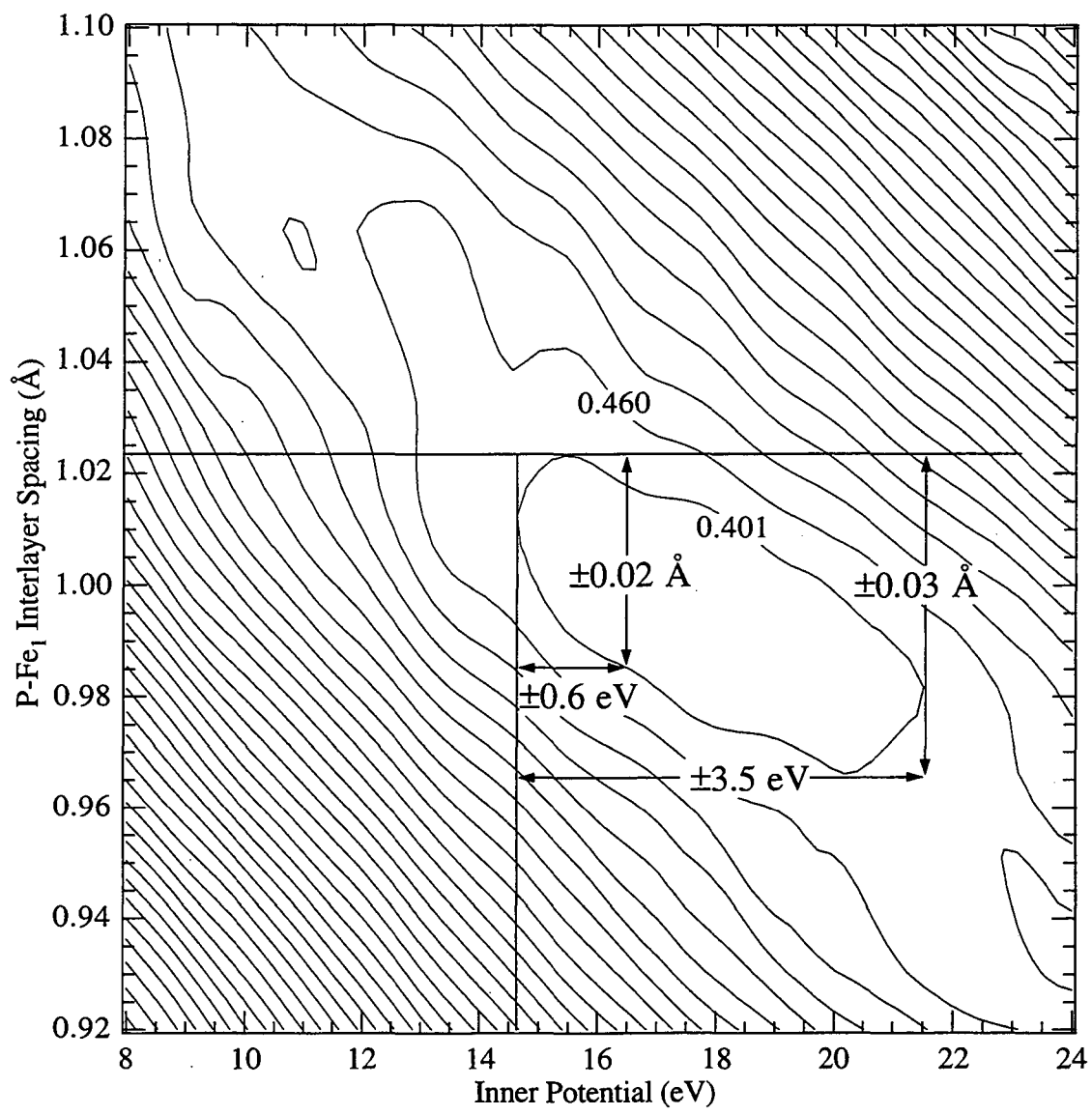


Figure 5

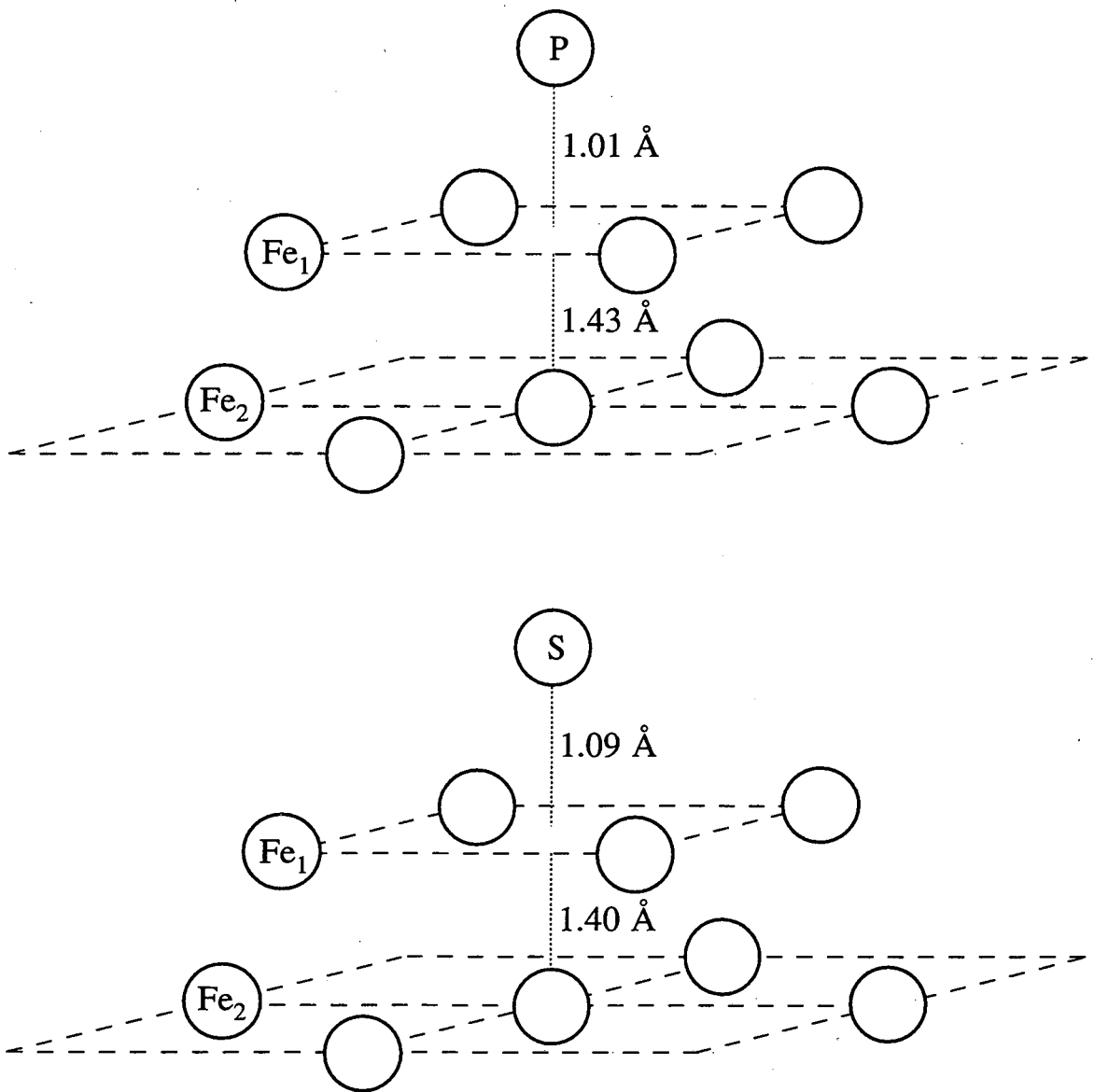


Figure 6

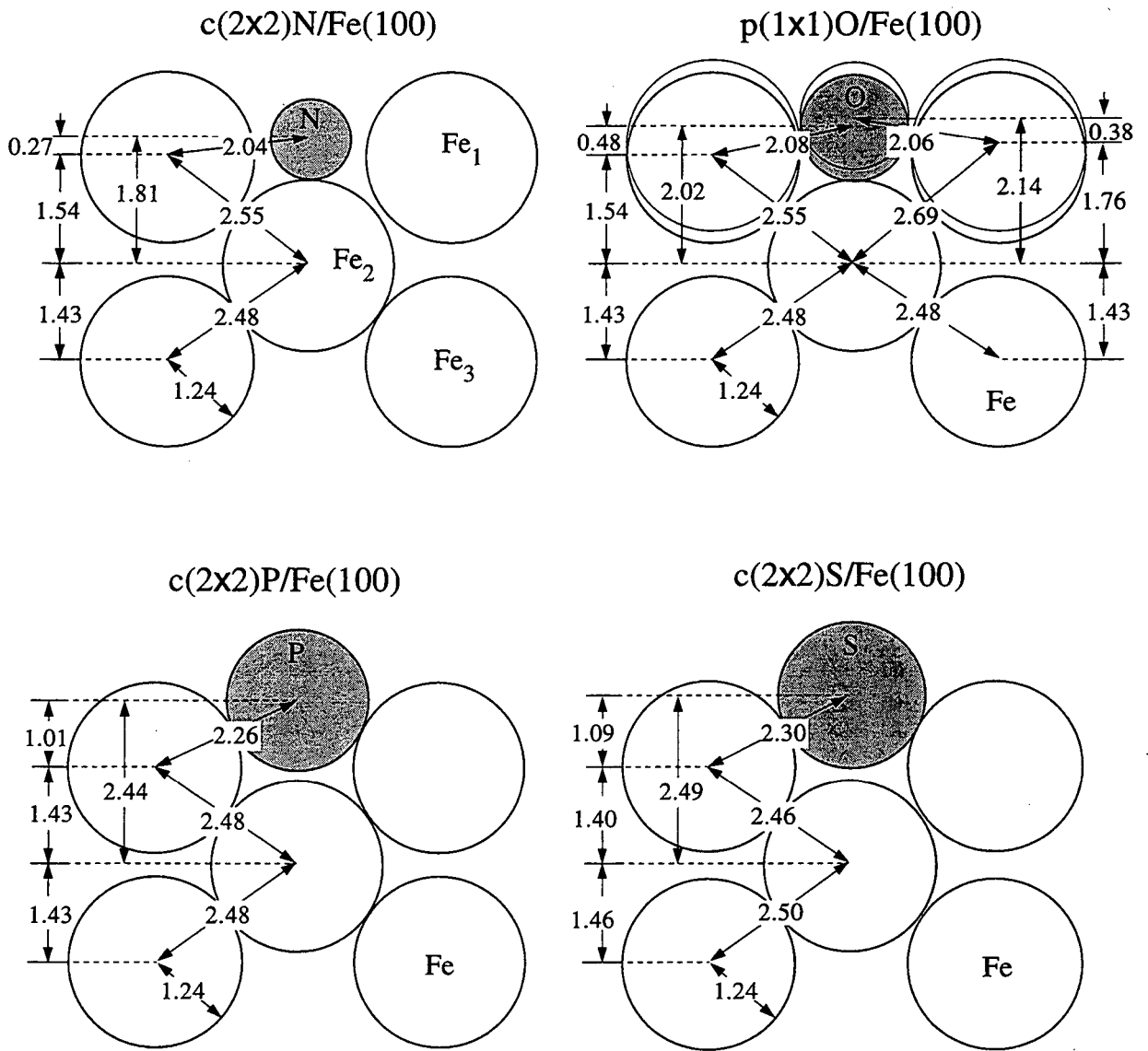


Figure 7

## REFERENCES

- <sup>1</sup>G.L. Krasko and G.B. Olson, *Solid State Commun.* **76**, 247(1990).
- <sup>2</sup>R. Wu, A.J. Freeman and G.B. Olson, *J. Mater. Res.* **7**, 2403(1992).
- <sup>3</sup>S. Tang, A.J. Freeman and G.B. Olson, *Phys. Rev. B* **47**, 2441(1993).
- <sup>4</sup>R. Wu, A.J. Freeman and G.B. Olson, *Phys. Rev. B* **47**, 6855(1993).
- <sup>5</sup>R. Wu, A.J. Freeman and G.B. Olson, *Phys. Rev. B* **50**, 75(1994).
- <sup>6</sup>B. Egert and G. Panzner, *Surf. Sci.* **118**, 345(1982).
- <sup>7</sup>S. Ohnishi, A.J. Freeman and M. Weinert, *Phys. Rev. B* **28**, 6741(1983).
- <sup>8</sup>Y. Sakisaka, Y.N. Rhodin, B. Egert and H. Grabke, *Solid State Commun.* **49**, 579(1984).
- <sup>9</sup>C.L. Fu and A.J. Freeman, *Phys. Rev. B* **35**, 925(1987).
- <sup>10</sup>S.R. Chubb and W.E. Pickett, *Phys. Rev. B* **38**, 10227(1988).
- <sup>11</sup>R. Wu and A.J. Freeman, *Phys. Rev. B* **47**, 3904(1993).
- <sup>12</sup>R. Imbihl, R.J. Behm, G. Ertl and W. Moritz, *Surf. Sci.* **123**, 129(1982).
- <sup>13</sup>K.O. Legg, F. Jona, D.W. Jepsen and P.M. Marcus, *Phys. Rev. B* **16**, 5271(1977).
- <sup>14</sup>S.R. Chubb and W.E. Pickett, *Solid State Commun.* **62**, 19(1987).
- <sup>15</sup>K.O. Legg, F. Jona, D.W. Jepsen and P.M. Marcus, *Surf. Sci.* **66**, 25(1977).
- <sup>16</sup>R.A. DiDio, E.W. Plummer and W.R. Graham, *J. Vac. Sci. Technol.* **A2**, 983(1984).
- <sup>17</sup>X.S. Zhang, L.J. Terminello, S. Kim, Z.Q. Huang, A.E. Schach von Wittenau and D.A. Shirley, *J. Chem. Phys.* **89**, 6538(1988).
- <sup>18</sup>D.P. Woodruff, D. Norman, B.W. Holland, N.V. Smith, H.H. Farrell and M.M. Traum, *Phys. Rev. Lett.* **41**, 1130(1978).
- <sup>19</sup>J.J. Barton, C.C. Bahr, S.W. Robey, Z. Hussain, E. Umbach and D.A. Shirley, *Phys. Rev. B* **34**, 3807(1986).
- <sup>20</sup>S.W. Robey, J.J. Barton, C.C. Bahr, G. Liu and D.A. Shirley, *Phys. Rev. B* **35**, 1108(1987).
- <sup>21</sup>L.J. Terminello, K.T. Leung, Z. Hussain, T. Hayashi, X.S. Zhang and D.A. Shirley, *Phys. Rev. B* **41**, 12787(1990).
- <sup>22</sup>L.Q. Wang, A.E. Schach von Wittenau, L.S. Wang Z.G. Ji, Z.Q. Huang and D.A. Shirley, *Phys. Rev. B* **44**, 1292(1991).
- <sup>23</sup>Z.Q. Huang, Z. Hussain, W.T. Huff, E.J. Moler and D.A. Shirley, *Phys. Rev. B* **48**, 1696(1993).
- <sup>24</sup>Z.Q. Huang, L.Q. Wang, A.E. Schach von Wittenau, Z. Hussain and D.A. Shirley, *Phys. Rev. B* **47**, 13626(1993).

- <sup>25</sup>J.J. Barton, C.C. Bahr, Z. Hussain, S.W. Robey, J.G. Tobin, L.E. Klebanoff and D.A. Shirley, *Phys. Rev. Lett.* **51**, 272(1983).
- <sup>26</sup>J.J. Barton, Z. Hussain and D.A. Shirley, *Phys. Rev. B* **35**, 933(1987).
- <sup>27</sup>S.D. Kevan, *Ph.D. Thesis*, The University of California, Berkeley, LBL-11017(1980).
- <sup>28</sup>Z. Hussain, E. Umbach, D.A. Shirley, J. Stohr and J. Feldhaus, *Nucl. Instrum. Methods* **195**, 115(1982).
- <sup>29</sup>C.A. Shell and J.C. Rivière, *Surf. Sci.* **40**, 1496(1973).
- <sup>30</sup>J.J. Barton, *Ph.D. Thesis*, The University of California, Berkeley, LBL-19215(1985).
- <sup>31</sup>J.J. Barton, S.W. Robey and D.A. Shirley, *Phys. Rev. B* **34**, 778(1986).
- <sup>32</sup>Y. Zheng and D.A. Shirley, *Chem. Phys. Lett.* **203**, 114(1993).
- <sup>33</sup>Y. Chen, H. Wu and D.A. Shirley, *CWMS Code - Unpublished*(1995).
- <sup>34</sup>J.J. Rehr and R.C. Albers, *Phys. Rev. B* **41**, 8139(1990).
- <sup>35</sup>A. Kaduwela, *Ph.D. Thesis*, University of Hawaii at Manoa, Honolulu(1991).
- <sup>36</sup>M. Sagurton, E.L. Bullock and C.S. Fadley, *Surf. Sci.* **182**, 287(1987).
- <sup>37</sup>R.E. Allen, G.P. Alldredge and F.W. de Wette, *J. Chem. Phys.* **54**, 2605(1971).
- <sup>38</sup>V.L. Moruzzi, J.F. Janak and A.R. Williams, *Calculated Electronic Properties of Metals*, (Pergamon Press, Inc., New York, 1978).
- <sup>39</sup>S. Tanuma, C.J. Powell and D.R. Penn, *Surf. Interface Anal.* **20**, 77(1993).
- <sup>40</sup>W.H. Press, S.A. Teukolsky, W.T. Vetterling and B.P. Flannery, *Numerical Recipes in Fortran: The Art of Scientific Computing*, 2 ed., (University Press, Cambridge, 1992).
- <sup>41</sup>J.C. Slater, *Phys. Rev.* **81**, 385(1951).
- <sup>42</sup>K.H. Johnson, *J. Chem. Phys.* **45**, 3085(1966).
- <sup>43</sup>K.H. Johnson, *Adv. Quantum Chem.* **7**, 143(1972).
- <sup>44</sup>M. Cook and M. Karplus, *J. Chem. Phys.* **72**, 7(1980).
- <sup>45</sup>D.A. Case, M. Cook and M. Karplus, *J. Chem. Phys.* **73**, 3294(1980).
- <sup>46</sup>M.E. Eberhart, K.H. Johnson and D. Adler, *Phys. Rev. B* **26**, 3138(1982).
- <sup>47</sup>J.S.-Y. Chao and K.D. Jordan, *J. Phys. Chem.* **91**, 5578(1987).
- <sup>48</sup>M. Cook and C.T. White, *Phys. Rev. B* **38**, 9674(1988).
- <sup>49</sup>H. Adachi and M. Takano, *J. Solid State Chem.* **93**, 556(1991).
- <sup>50</sup>J.C. Slater, *Solid State and Molecular Theory: A Scientific Biography*, (Wiley, New York, 1975).
- <sup>51</sup>Jr. J.G. Norman, *Mol. Phys.* **31**, 1191(1976).
- <sup>52</sup>K. Schwarz, *Phys. Rev. B* **5**, 2466(1972).
- <sup>53</sup>K.A.R. Mitchell, *Surf. Sci.* **100**, 225(1980).

LAWRENCE BERKELEY NATIONAL LABORATORY  
UNIVERSITY OF CALIFORNIA  
TECHNICAL & ELECTRONIC INFORMATION DEPARTMENT  
BERKELEY, CALIFORNIA 94720